Supporting Information

Uncovering precursors for VOC production from ozonolysis of seawater

Frances E. Hopkins[1*], Daniel P. Phillips[1,2,3], Yinghao Chen, Peter S. Liss[2], Mingxi Yang[1]

[1]Plymouth Marine Laboratory, Plymouth, PL1 3DH, U.K.

[2] Centre for Ocean and Atmospheric Sciences, School of Environmental Sciences, University if East Anglia, Norwich, NR4 7TJ, U.K.

[3] National Oceanography Centre, National Oceanography Centre, European Way, Southampton, UK

*Correspondence to fhop@pml.ac.uk

Methods

Seawater sampling

Surface seawater was routinely collected from the Western Channel Observatory station L4 using the rosette on the RV *Plymouth Quest* at a mean depth of **1.8 ± 0.3 m** (range: **1.4 m**) between **08:00–10:00** local time. Seawater was transferred directly from Niskin bottles into acid-washed, thoroughly rinsed glass bottles using Tygon tubing and gas-sensitive techniques. Bottles were allowed to overflow **3×** before sealing with a ground-glass stopper, minimizing bubbles and gas loss. Samples were transported to the laboratory in a dark, insulated cool box and analysed as soon as possible to limit DOM alteration (**59%** within **3 h**, **94%** within **24 h**).

Sampling campaigns covered contrasting seasons:

- **Late winter/spring:** 14 Feb 2017 – 03 May 2017
- **Autumn/winter:** 04 Sep 2018 – 05 Nov 2018
- **Summer/autumn:** 15 Jun 2020 – 12 Oct 2020

Bubble-column reactor

Experiments used a custom 1.45 L cylindrical borosilicate glass column fitted with a fine glass-frit sparger (acid-washed and rinsed with ultrapure water between samples) (Figure S1). A ~200 mL volume below the sparger housed a gas inlet and stopcock. With the stopcock closed, **1.2 L** of sample was siphoned above the sparger using silicone tubing to minimize bubble formation, leaving a **205 mL** headspace containing the gas outlet.

Compressed artificial air (BOC BTCA 178) served as the carrier gas and was scrubbed for organics via a custom Pt catalyst at **450 °C**. A flow of **150 n mL min⁻¹** (1 atm, 0 °C; ≈ **165 mL min⁻¹** at room temperature) was set with mass-flow controllers (Bronkhorst EL-FLOW Select series). Opening the stopcock directed the gas through the frit, producing a dense turbulent plume of bubbles (~**0.5 mm** diameter each; ~**3 mL** total bubble volume) rising through the sample. Bubble residence time in water was ~**1.2 s**.

The total bubble–water interfacial area, A (cm²), was estimated as:

$$A = \frac{3V}{r}$$

where V is the total bubble displacement volume and r the radius of an individual bubble (from column photos with a ruler reference). Notably, A cancels the VOC production ratio (see Eq. S4), so uncertainty in A does not affect that ratio.

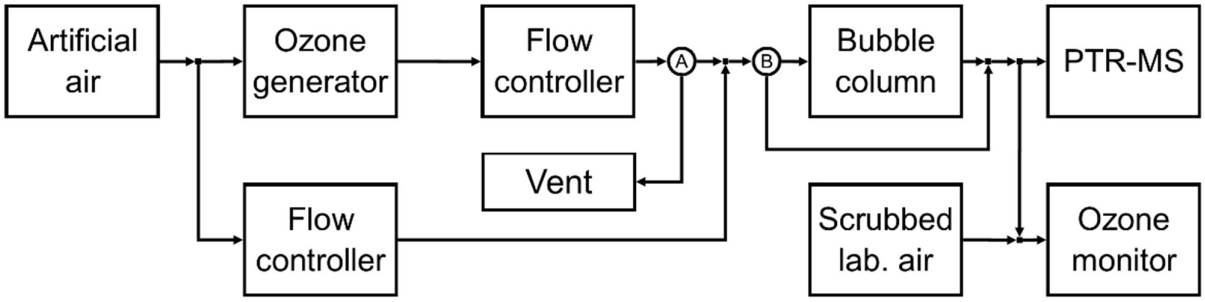

Figure S1. Schematic of the turbulent ozonolysis experimental setup. Arrows indicate flow; A and B denote three-way valves.

Ozone generation and measurement

O_3 was generated from the artificial air using a corona-discharge source (Enaly 1000BT-12) and mixed into the carrier stream to achieve **1–15 ppmv** (rarely >3 ppmv). Although these O_3 levels exceed typical marine boundary layer (MBL) values (×25–150), the response was experimentally linear below ~**4 ppmv**. Headspace O_3 was measured with a dual-channel (simultaneous blank correction) monitor (2B Technologies Model 205), providing high temporal resolution. The monitor's inlet draws ~**2 L min⁻¹**; to supply the balance, a tee provided additional O_3-scrubbed dilution air vented to the lab, yielding an effective dilution of ~**93–98%** and necessitating elevated inlet O_3 concentrations. Total flows (monitor + dilution air) were verified with a digital bubble meter (Gilian Gilibrator-2). The O_3 generator and monitor were warmed for **1–2 h** with artificial air to stabilize. PFA tubing (3.2 mm ID) connected the O_3 generator to the column and the column to the monitor; three-way valves and MFCs were stainless steel.

PTR-MS measurements

Headspace VOCs were quantified with a PTR-MS. All line connections between column headspace and instrument were 3.2 mm ID PFA. Core monitored masses included methanol (*m/z* 33), acetaldehyde (*m/z* 45), acetone (*m/z* 59), DMS (*m/z* 63), and isoprene (*m/z* 69). Additional masses varied by campaign (Table S1); details of masses, fragment ion ratios from literature, and dwell times are provided in Table S2. For isoprene, *m/z* 39 and 41 (fragments) were included (Schwarz et al., 2009). Overall temporal resolution was 3.1–7.7 s (0.13–0.27 Hz). Internally corrected PTR-MS mixing ratios (ppbv) were used. Method parameters are in Table S3.

Table S1. PTR-MS measurement frequencies, temporal resolutions and mass list by campaign.

Campaign	Frequency (Hz)	Time (s)	Notes
2017	0.13	7.7	Added *m/z* 21, 32, 33, 39, 42, 42, 43, 45, 47, 59, 60, 61, 63, 69, 71, 79, 93, 107, 137
2018 beginning	0.32	3.1	Removed *m/z* 39, 42, 43, 47, 60, 61, 71, 79, 93, 107, 137 Added *m/z* 37
2018 end	0.27	3.7	Added *m/z* 39 with increased dwell time Increased *m/z* 32 and 37 dwell times
2020 beginning	0.16	6.2	Added *m/z* 43, 47, 57, 61, 73
2020 end	0.14	7.2	Added *m/z* 55, 87

Table S2. Target masses, expected compounds, literature ion ratios, formulas, and dwell times [1,2].

Mass-charge ratio	Expected compound/s	Literature ion ratio (%)	Structural formula	Residence time (ms)
21	Hydronium	-	$H_3{}^{18}O^+$	50
32	Oxygen	-	$O_2{}^+$	20–50
33	Methanol	100[b]	$CH_3OH_2{}^+$	500
37	Water dimer	-	$H_2O.H_3O^+$	20–50
39	Isoprene (fragment) Isotopic water dimer Pentanal (fragment)	10[b] - 2[b]	CH_2CCH^+ $H_2{}^{18}O.H_3O^+$ / $H_2O.H_3{}^{18}O^+$	50–500
41	Isoprene (fragment) Propanal (fragment) Pentanal (fragment)	39[b] 4[b] 23[b]	$CH_2CCH_3{}^+$	500
43	Propene Acetone (fragment)	- 10[a]		500
45	Acetaldehyde Pentanal	100[b] 2[b]	$CH_3COOH_2{}^+$	500
47	Formic acid	-		500
55	Butanal (fragment) Butadiene	57[a], 90[b] -		
57	Butene	100[a]		500
59	Acetone Propanal	90[a], 98[b] 100[a], 89[b]	$CH_3COCH_3{}^+$ $CH_3CH_2CH_2O^+$	500
61	Acetic acid	-		500
63	DMS	100[a]	$CH_3SHCH_3{}^+$	500
69	Isoprene Pentanal (fragment)	100[a],46[b] 78[a], 68[b]	$CH_2C(CH_3)CHCH_3{}^+$	500
73	Butanal Butanone	43[a], 7[b] -	C4H8O	500
87	Pentanal Pentanone	87[a], 5[b], 100[a]		500

Table S3. PTR-MS method parameters.

Parameter	Value
Drift chamber pressure (mBar)	2.21
Drift chamber voltage (true) (V)	690
Drift chamber temperature (°C)	80
H_2O mass flow controller (mL min^{-1})	5
Inlet flow rate (mL min^{-1})	80–120
Inlet temperature (°C)	80

Experimental Sequence

Each experiment cycled through four stages, with O_3 and VOCs measured continuously:

1. **Stage 1 — O_3 input:** Bypass column to measure generator output (O_3 input).
2. **Stage 2 — Dry VOC blank:** Bypass column for a gas-phase VOC blank.
3. **Stage 3 — Air purge:** Pass artificial air through the water sample. This strips dissolved VOCs to the headspace and flushes the headspace to an approximate steady state with the underlying water. Of the monitored VOCs, only isoprene typically declines appreciably during this stage due to its low solubility and efficient purging.
4. **Stage 4 — Oxidation:** Add O_3 to the carrier stream to initiate ozonolysis.

Typically, two Milli-Q water runs were performed prior to triplicate seawater samples to verify column cleanliness and provide a humid VOC blank.

Reactant-addition experiments

To probe precursor classes and product signatures, select reactants were added to **aged seawater** (stored ~**1 month**, dark, gas-tight glass, **20 °C**) in the bubble column. Aged seawater was preferred over Milli-Q to preserve salinity, which influences bubble size distributions and thus gas–liquid interfacial area and reaction rates (FwarnF, 1975).

- **Phytoplankton:** *Emiliania huxleyi* Rutgers 607 was grown on-site to senescence (mature, not lysing) and added directly by briefly removing the column cap (~**10 s**) and pipetting **5–20 mL** culture onto the water surface. Dilutions targeted final cell abundances within ambient seawater ranges (assuming no algal cells in the aged seawater).
- **NOM:** Suwannee River natural organic matter (International Humic Substances Society) was dissolved in **10 mL** aged seawater and poured into the column to yield **0–10 mg L^{-1}**.

- **Fatty acids:** Oleic and nonanoic acids (**0–400 µL**) were injected directly onto the water surface via the column side arm.

- **Iodide:** KI (Acros Organics, >99%) was dissolved in Milli-Q to prepare a **0.6 mM** I^- standard (serial dilution). Aliquots (**0–500 µL**) were injected into the seawater; aged seawater was avoided as solvent to minimize background I^-. Natural surface seawater I^- is ~**100 nM** [3]; each **100 µL** addition here increased [I^-] by **50.1 nM**.

Calibration

VOC data were averaged to 1 min intervals and converted using calibration factors derived from gas-phase calibrations with a certified standard (Apel-Riemer Environmental, 500 ppbv for all VOCs here). O_3 data were also 1-min averaged, corrected for zero drift, and adjusted for the scrubbed dilution air. The O_3 monitor was calibrated during routine servicing, cross-checked against other instruments, or verified with a portable O_3 source (2B Technologies Model 306). Under standard operation, calibration drift was negligible.

Table S4. Instrument calibration factors.

Instrument	Compound	Calibration factor
PTR–MS	Methanol	0.447±0.053
	Acetaldehyde	0.820±0.042
	Acetone	0.949±0.103
	DMS	0.549±0.146
	Isoprene	0.138±0.012
O_3 monitor	O_3	n/a, frequently updated with internal correction

Data processing

Peak data

Figure S2 shows a representative time series (1-min resolution) for acetaldehyde, acetone, isoprene, and O_3 during ozonolysis of one sample; similar plots were used to extract peak metrics.

We define two primary metrics from **Stage 4**:

- **VOC peak height (ppbv):** The difference between the steady-state headspace concentration at the end of Stage 3 and the maximum concentration during Stage 4.

- **Initial gradient (ppbv s^{-1}):** The maximum initial rate of increase prior to the peak maximum, obtained by linear regression over the earliest, linear segment.

The area under the peak corresponds to the total VOC produced from the available DOM; however, full consumption typically required **>1.5 h**, so peak area was seldom integrated to maintain O_3-input stability. The small apparent step in peak height between ~14:50–14:51 in Figure S2, relative to the

initial slope (green line), is an artefact of 1-min averaging rather than reaction kinetics (see Sect. 2.5.3).

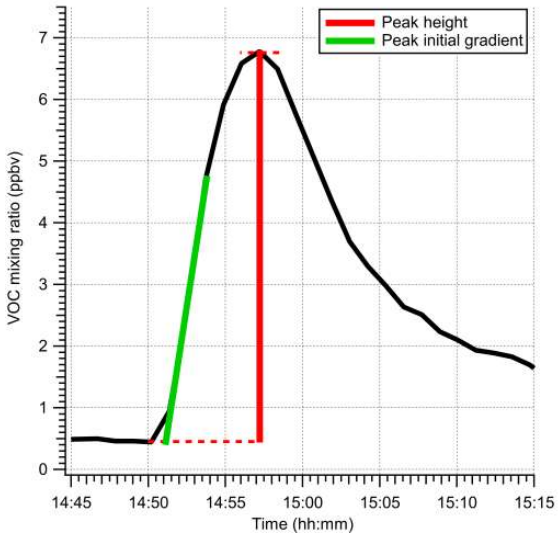

Figure S2. Example determination of VOC peak height and initial gradient.

Headspace mass balance and production rate

The headspace concentration of a VOC is governed by production at the air–water interface and advective removal by the purge flow. The differential equation is:

$$\frac{dC_{\mathrm{VOC}}}{dt} = \frac{P_{\mathrm{VOC}}\, A_{\mathrm{bub}}}{V_{\mathrm{air}}} - \frac{F_{\mathrm{air}}}{V_{\mathrm{air}}}\, C_{\mathrm{VOC}} \qquad \text{(S1)}$$

where $C_{(\mathrm{VOC})}$ is the headspace concentration (ppbv), $P_{(\mathrm{VOC})}$ is the areal production flux (mol m^{-2} s^{-1}), $A_{(\mathrm{bub})}$ is interfacial area (m^2), $V_{(\mathrm{air})}$ is headspace volume (m^3), and $F_{(\mathrm{air})}$ is the gas flow (m^3 s^{-1}).

At the earliest times of Stage 4, $C_{(\mathrm{VOC})}$ is still small, so the purge-loss term is minor. Thus,

$$P_{\mathrm{VOC}} \approx \frac{V_{\mathrm{air}}}{A_{\mathrm{bub}}} \left(\frac{dC_{\mathrm{VOC}}}{dt}\right)_{\mathrm{initial}} \qquad \text{(S2)}$$

O_3 deposition flux

O_3 is supplied at a constant inlet concentration, and the deposition flux into the sample is:

$$D_{F,\mathrm{O_3}} = \frac{F_{\mathrm{air}}\left(C_{\mathrm{O_3},G} - C_{\mathrm{O_3},H}\right)}{A_{\mathrm{bub}}} \approx \frac{F_{\mathrm{air}}\, C_{\mathrm{O_3},G}}{A_{\mathrm{bub}}} \text{(early times; O}_3\text{ limiting)} \qquad \text{(S3)}$$

where $C_{(O_3,G)}$ and $C_{(O_3,H)}$ are inlet and headspace O_3, respectively. Early in Stage 4, headspace $O_3 \approx 0$ when DOM or reduced sulfur species rapidly consume O_3, justifying the approximation. Wall losses on stainless steel, glass, and PFA are assumed negligible relative to sample uptake.

VOC–O_3 production ratio

Dividing Eq. S2 by Eq. S3 yields a dimensionless "production ratio" of VOC produced per O_3 taken up:

$$\frac{P_{\mathrm{VOC}}}{D_{F,\mathrm{O_3}}} \approx \frac{V_{\mathrm{air}}}{F_{\mathrm{air}}} \frac{(dC_{\mathrm{VOC}}/dt)_{\mathrm{initial}}}{C_{\mathrm{O_3},G}} \qquad \text{(S4)}$$

Note: $A_{(\mathrm{bub})}$ cancels, so uncertainty in interfacial area does not affect this ratio.

DMS purge and oxidation losses

When DMS levels were high, O_3 was not detected in the headspace until a substantial fraction of DMS had been removed. The DMS loss rate during Stage 3 (air purge only) and Stage 4 (purge + oxidation) was quantified by linear regression; the **oxidative** loss rate was taken as:

$$\left(\mathrm{loss}_{\mathrm{Stage\,4}}\right) - \left(\mathrm{loss}_{\mathrm{Stage\,3}}\right)$$

References

1 Warneke, C., De Gouw, J. A., Kuster, W. C., Goldan, P. D. & Fall, R. Validation of atmospheric VOC measurements by proton-transfer-reaction mass spectrometry using a gas-chromatographic preseparation method. *Environmental science & technology* **37**, 2494-2501 (2003).

2 Schwarz, K., Filipiak, W. & Amann, A. Determining concentration patterns of volatile compounds in exhaled breath by PTR-MS. *Journal of Breath Research* **3**, 027002 (2009).

3 Chance, R., Baker, A. R., Carpenter, L. & Jickells, T. D. The distribution of iodide at the sea surface. *Environmental Science: Processes & Impacts* **16**, 1841-1859 (2014).

Data

Table S5. VOC data (ppbv) presented in Figure 1

Timestamp_ave	me45_ave	me59_ave	me69_ave
05/11/2018 14:25	2.144	1.116	0.104
05/11/2018 14:26	1.873	0.911	0.093
05/11/2018 14:28	1.265	0.619	0.079
05/11/2018 14:29	1.088	0.529	0.077
05/11/2018 14:30	0.984	0.474	0.069
05/11/2018 14:31	0.901	0.444	0.075
05/11/2018 14:32	9.535	5.858	0.453
05/11/2018 14:33	9.670	2.604	0.603
05/11/2018 14:35	9.637	2.220	0.588
05/11/2018 14:36	9.934	2.258	0.583
05/11/2018 14:37	10.014	2.554	0.583
05/11/2018 14:38	9.756	2.869	0.592
05/11/2018 14:39	9.380	3.086	0.576
05/11/2018 14:40	8.763	3.281	0.544
05/11/2018 14:42	7.813	3.416	0.527
05/11/2018 14:43	7.098	3.557	0.551
05/11/2018 14:44	6.513	3.475	0.487
05/11/2018 14:45	6.271	3.584	0.492
05/11/2018 14:46	6.028	3.482	0.499
05/11/2018 14:47	5.796	3.485	0.461
05/11/2018 14:49	5.781	3.561	0.460
05/11/2018 14:50	5.581	3.494	0.443
05/11/2018 14:51	5.680	3.885	0.945
05/11/2018 14:52	6.223	5.014	2.660
05/11/2018 14:53	6.666	5.500	4.699
05/11/2018 14:54	7.087	5.289	5.914
05/11/2018 14:56	7.280	4.889	6.585
05/11/2018 14:57	7.322	4.635	6.781
05/11/2018 14:58	7.301	4.449	6.497
05/11/2018 14:59	7.328	4.247	5.776
05/11/2018 15:00	7.290	4.276	5.067
05/11/2018 15:01	6.997	4.118	4.358
05/11/2018 15:03	6.777	4.020	3.697
05/11/2018 15:04	6.677	3.959	3.299
05/11/2018 15:05	6.624	3.883	2.980
05/11/2018 15:06	6.453	3.722	2.635
05/11/2018 15:07	6.332	3.701	2.510
05/11/2018 15:08	6.339	3.669	2.236
05/11/2018 15:10	6.193	3.601	2.100
05/11/2018 15:11	6.235	3.618	1.934
05/11/2018 15:12	6.145	3.623	1.888
05/11/2018 15:13	6.115	3.567	1.829

05/11/2018 15:14	5.753	3.354	1.694
05/11/2018 15:15	5.536	3.189	1.473
05/11/2018 15:17	5.088	2.957	1.335
05/11/2018 15:18	4.882	2.810	1.256
05/11/2018 15:19	4.716	2.674	1.120
05/11/2018 15:20	4.560	2.667	1.115
05/11/2018 15:21	4.632	2.741	1.043
05/11/2018 15:22	4.579	2.658	1.015
05/11/2018 15:24	4.528	2.614	0.978
05/11/2018 15:25	4.465	2.649	0.978
05/11/2018 15:26	4.492	2.553	0.921
05/11/2018 15:27	4.392	2.576	0.914
05/11/2018 15:28	4.356	2.577	0.889
05/11/2018 15:29	4.252	2.497	0.855
05/11/2018 15:31	3.857	3.250	0.441
05/11/2018 15:32	2.508	1.888	0.132
05/11/2018 15:33	2.616	1.664	0.115
05/11/2018 15:34	2.256	1.276	0.095
05/11/2018 15:35	2.085	1.120	0.098
05/11/2018 15:36	1.917	0.968	0.085
05/11/2018 15:38	1.849	0.903	0.090
05/11/2018 15:39	1.543	0.798	0.084
05/11/2018 15:40	1.036	0.557	0.077

Table S6. Ozone data (ppbv) presented in Figure 1

Time_1min	O3_ppb_1min
05/11/2018 14:25	2118.41
05/11/2018 14:26	2121.49
05/11/2018 14:27	1594.86
05/11/2018 14:28	32.7017
05/11/2018 14:29	35.7829
05/11/2018 14:30	8.05217
05/11/2018 14:31	-8.6376
05/11/2018 14:32	21.404
05/11/2018 14:33	7.28188
05/11/2018 14:34	-14.0297
05/11/2018 14:35	16.7822
05/11/2018 14:36	-0.934627
05/11/2018 14:37	-21.2191
05/11/2018 14:38	46.0535
05/11/2018 14:39	-3.75905
05/11/2018 14:40	-13.7729
05/11/2018 14:41	-28.6653
05/11/2018 14:42	-32.2601
05/11/2018 14:43	16.7822
05/11/2018 14:44	-18.1379

05/11/2018 14:45	8.30894
05/11/2018 14:46	2.40333
05/11/2018 14:47	-10.1782
05/11/2018 14:48	-15.827
05/11/2018 14:49	-2.98875
05/11/2018 14:50	37.0667
05/11/2018 14:51	28.0799
05/11/2018 14:52	2.91686
05/11/2018 14:53	26.0258
05/11/2018 14:54	2.40333
05/11/2018 14:55	17.2957
05/11/2018 14:56	66.5948
05/11/2018 14:57	63.2568
05/11/2018 14:58	70.4463
05/11/2018 14:59	114.353
05/11/2018 15:00	106.907
05/11/2018 15:01	128.475
05/11/2018 15:02	177.261
05/11/2018 15:03	220.654
05/11/2018 15:04	226.56
05/11/2018 15:05	212.181
05/11/2018 15:06	237.858
05/11/2018 15:07	287.157
05/11/2018 15:08	296.657
05/11/2018 15:09	282.535
05/11/2018 15:10	287.157
05/11/2018 15:11	313.603
05/11/2018 15:12	359.051
05/11/2018 15:13	341.591
05/11/2018 15:14	366.497
05/11/2018 15:15	249.155
05/11/2018 15:16	141.57
05/11/2018 15:17	40.9182
05/11/2018 15:18	61.4595
05/11/2018 15:19	11.3901
05/11/2018 15:20	-5.55641
05/11/2018 15:21	-18.3947
05/11/2018 15:22	-10.6917
05/11/2018 15:23	-14.8
05/11/2018 15:24	23.2014
05/11/2018 15:25	-42.7874
05/11/2018 15:26	-18.9082
05/11/2018 15:27	-16.3406
05/11/2018 15:28	-31.7465
05/11/2018 15:29	0.605967
05/11/2018 15:30	-5.81318
05/11/2018 15:31	-15.0567
05/11/2018 15:32	137.462

05/11/2018 15:33	1958.96
05/11/2018 15:34	2029.31
05/11/2018 15:35	2040.35
05/11/2018 15:36	2063.98
05/11/2018 15:37	2136.13
05/11/2018 15:38	2118.92
05/11/2018 15:39	2027.26

Table S7. PTR-MS data presented in Figure 2a and 2b (m/z 45, 49, 69 = peak height, m/zXX_grad = peak gradient, m/zXX_gradSD = standard devaition)

DoY	m/z45	m/z45_SD	m/z59_	m/z59_SD	m/z69	m/z69_SD	m/z45_grad	m/z45_gradSD	m/z59_grad	m/z59_gradSD	m/z69_grad	m/z69_gradSD
45	2.038	0.192	2.41	1.358	8.935	4.425	0.0151	0.0059	0.0164	0.0034	0.1247	0.0234
51	2.31	0.602	1.972	0.606	7.225	2.22	0.0165	0.002	0.0234	0.0106	0.0519	0.0191
60	2.144	0.25	1.219	0.144	5.489	1.424	0.0193	0.0004	0.0152	0.0019	0.0557	0.0179
65	2.119	0.562	1.09	0.263	11.047	8.426	0.0186	0.0077	0.0174	0.0046	0.0556	0.0232
73	2.972	0.629	1.614	0.282	5.018	1.345	0.0265	0.0017	0.0137	0.0014	0.0536	0.0147
86	3.132	0.426	1.307	0.249	5.143	0.333	0.0153	0.0012	0.0142	0.0035	0.0523	0.0121
93	2.718	0.625	2.659	0.242	11.25	1.787	0.016	0.0026	0.0324	0.0113	0.088	0.0152
100	3.955	0.75	4.177	1.623	15.299	7.401	0.0211	0.0054	0.045	0.0038	0.1835	0.0911
108	3.117	0.303	6.886	1.947	17.8	2.639	0.0185	0.0056	0.056	0.0158	0.1896	0.0584
114	4.696	0.115	6.722	0.427	8.787	0.274	0.0248	0.0017	0.0539	0.0028	0.0834	0.0211
122	5.807	1.051	15.477	1.311	30.994	5.812	0.0262	0.0069	0.1188	0.0016	0.2864	0.0014
246	1.637	0.207	5.763	1.323	73.75	7.653	0.0048	0.0019	0.0309	0.0015	0.1521	0.0179
253	2.757	0.424	1.593	0.418	85.071	10.635	0.0063	0.002	0.0077	0.0028	0.146	0.0132
267	1.809	0.18	3.108	0.94	48.9	10.317	0.0038	0.0006	0.0143	0.0045	0.0809	0.0061
281	2.455	0.013	2.419	0.789	54.948	5.402	0.0091	0.0018	0.0131	0.0038	0.1654	0.0104
290	3.164	0.483	2.417	0.088	48.202	8.949	0.0117	0.0012	0.0289	0.0095	0.2704	0.0615
295	3.538	0.219	1.945	0.215	40.841	2.168	0.0123	0.0018	0.0157	0.0062	0.2367	0.0157
309	2.405	0.569	1.758	0.433	44.003	13.291	0.0093	0.0012	0.0109	0.002	0.1845	0.0295
167	2.285	0.456	3.732	0.217	9.401	3.993	0.0106	0.0011	0.0247	0.0038	0.0385	0.0128
175	2.047	0.296	3.449	0.909	11.478	3.48	0.0059	0.0015	0.0199	0.0066	0.0454	0.0156
189	1.489	0.008	2.926	0.166	13.419	1.607	0.0062	0.0013	0.0191	0.0033	0.0611	0.0028
196	1.53	0.194	4.154	0.404	12.535	1.457	0.0033	0.0008	0.0196	0.003	0.041	0.0077
202	1.611	0.395	2.763	0.225	9.623	5.918	0.0056	0	0.0139	0.0029	0.0302	0.0102
210	1.884	0.107	4.028	1.044	22.135	10.39	0.0065	0.001	0.0253	0.0081	0.0889	0.0511
216	1.311	0.321	2.672	0.669	10.201	2.859	0.0038	0.0012	0.0121	0.0021	0.0311	0.0041
223	2.574	0.107	3.64	0.955	19.882	15.169	0.0122	0.0027	0.0219	0.0033	0.0823	0.0318

230	2.022	0.15	2.415	0.151	6.828	1.325	0.0113	0.0028	0.0131	0.0046	0.0304	0.011
245	2.61	0.382	1.178	0.189	4.274	0.835	0.0138	0.0021	0.0043	0.0008	0.0099	0.0037
251	1.554	0.163	2.01	0.188	5.115	1.161	0.0084	0.0018	0.0077	0.0013	0.0133	0.0043
258	1.817	0.325	1.546	0.135	6.275	0.914	0.013	0.0002	0.0073	0.0008	0.0203	0.0045
265	2.295	0.273	1.839	0.39	8.647	0.319	0.0177	0.0029	0.0107	0.002	0.0366	0.0049
286	1.385	0.203	1.718	0.278	7.292	2.646	0.0081	0.0013	0.0099	0.0035	0.0281	0.0109

Table S8. Data presented in Figure 2c (xxx_prod = VOC production ratio, xxx_SD = standard deviation)

DoY	Aceta_prod	Aceta_SD	Aceto_prod	Aceto_SD	Isop_prod	Isop_SD
46	0.0002	0.0001	0.0002	0.0000	0.0016	0.0003
52	0.0002	0.0000	0.0003	0.0001	0.0006	0.0002
61	0.0003	0.0000	0.0002	0.0000	0.0008	0.0003
66	0.0003	0.0001	0.0002	0.0001	0.0008	0.0003
73	0.0004	0.0000	0.0002	0.0000	0.0008	0.0002
90	0.0002	0.0000	0.0002	0.0000	0.0007	0.0002
94	0.0002	0.0000	0.0004	0.0001	0.0011	0.0002
101	0.0002	0.0001	0.0005	0.0000	0.0021	0.0010
108	0.0003	0.0001	0.0008	0.0002	0.0026	0.0008
114	0.0003	0.0000	0.0006	0.0000	0.0010	0.0002
122	0.0003	0.0001	0.0016	0.0000	0.0038	0.0000
247	0.0005	0.0002	0.0031	0.0002	0.0152	0.0018
254	0.0005	0.0002	0.0006	0.0002	0.0118	0.0011
268	0.0003	0.0000	0.0010	0.0003	0.0056	0.0004
282	0.0002	0.0000	0.0003	0.0001	0.0041	0.0003
290	0.0005	0.0000	0.0011	0.0004	0.0105	0.0024
297	0.0004	0.0001	0.0006	0.0002	0.0085	0.0006
309	0.0006	0.0001	0.0007	0.0001	0.0111	0.0018
167	0.0005	0.0001	0.0011	0.0002	0.0018	0.0006
175	0.0003	0.0001	0.0008	0.0003	0.0019	0.0007
189	0.0002	0.0000	0.0005	0.0001	0.0017	0.0001
196	0.0004	0.0002	0.0016	0.0003	0.0034	0.0006
202	0.0003	0.0001	0.0010	0.0002	0.0021	0.0007
210	0.0006	0.0001	0.0022	0.0007	0.0077	0.0044
216	0.0003	0.0001	0.0008	0.0001	0.0022	0.0003
223	0.0009	0.0003	0.0019	0.0003	0.0071	0.0027
230	0.0009	0.0003	0.0012	0.0004	0.0027	0.0010
245	0.0013	0.0002	0.0004	0.0001	0.0010	0.0004
251	0.0008	0.0002	0.0007	0.0001	0.0013	0.0004
259	0.0007	0.0003	0.0005	0.0001	0.0014	0.0003
265	0.0011	0.0002	0.0006	0.0001	0.0022	0.0003
286	0.0004	0.0002	0.0004	0.0002	0.0012	0.0005

Table S9. Seasonal production ratio data presented in Figure 4

m/z 45	m/z 45SD	m/z 59	m/z 59SD	m/z 69	m/z 69SD	Seasons
0.000255	0.000078	0.000225	0.000036	0.000883	0.000352	Spring pre-bloom
0.000267	0.000054	0.000779	0.000457	0.002117	0.001149	Spring bloom
0.000343	0.000142	0.001243	0.000549	0.00225	0.0006	Early summer
0.001019	0.000183	0.000541	0.000134	0.0014	0.00046	Late summer
0.000418	0.000125	0.000712	0.000295	0.009531	0.003804	Autumn

Table S10. VOC peak height and production ratio of VOCs presented in Figure 5

m/z 45_peak	m/z 45_prod	m/z 59_peak	m/z 59_prod	m/z 69_peak	m/z 69_prod	Vol_culture (mL)
0	0	0	0	0	0	0
1.074	0.0000442	1.967	0.0000841	-0.406	0.0000445	5
2.044	0.00009	4.244	0.0001316	1.059	0.0000977	10
3.618	0.0001797	7.438	0.0002791	2.929	0.0001714	20